VIP Wearable Solar Cells Very Important Paper

DOI: 10.1002/ange.201407688

# A Lightweight Polymer Solar Cell Textile that Functions when Illuminated from Either Side**

*Zhitao Zhang, Xueyi Li, Guozhen Guan, Shaowu Pan, Zhengju Zhu, Dayong Ren, and Huisheng Peng**

***Abstract:*** *An all-solid-state, lightweight, flexible, and wearable polymer solar cell (PSC) textile with reasonable photovoltaic performance has been developed. A metal textile electrode made from micrometer-sized metal wires is used as the cathode, and the surfaces of the metal wires are dip-coated with the photoactive layers. Two ultrathin, transparent, and aligned carbon nanotube sheets that exhibit remarkable electronic and mechanical properties were coated onto the modified metal textile at both sides as the anode to produce the desired PSC textile. Because of the designed sandwich structure, the PSC textile displays the same energy conversion efficiencies regardless of which side it is irradiated from. As expected, the PSC textiles are highly flexible, and their energy conversion efficiencies varied by less than 3% after bending for more than 200 cycles. The PSC textile shows an areal density (5.9 mg cm$^{-2}$) that is lower than that of flexible film-based PSCs (31.3 mg cm$^{-2}$).*

Flexible electronic textiles have been widely recognized as a promising direction in the advancement of the next-generation electronics.[1–8] To this end, a lot of efforts have been made to develop fiber-shaped devices, such as solar cells, inspired by the advancement of the textile industry.[9–16] Dye-sensitized solar cells (DSCs) have been investigated particularly thoroughly because of an easy fabrication process and high energy conversion efficiencies. Unfortunately, fiber-shaped DSCs need to be sealed because of the use of liquid electrolytes, which is unfavorable as they thus lose their advantages in terms of being thin, lightweight, and wearable.[15,16] Gel electrolytes have been suggested to replace their liquid counterparts. However, the resulting fiber-shaped DSCs showed much lower energy conversion efficiencies. Furthermore, the energy conversion efficiencies substantially decreased with time. For both liquid and gel electrolytes, the fiber-shaped DSCs easily failed to work even after bending for only a few cycles owing to the low stability of the electrolyte. Alternately, fiber-shaped polymer solar cells (PSCs) were found to display higher stabilities than fiber-shaped DSCs because of their all-solid-state structure and have attracted increasing attention.[17–20]

Both fiber-shaped DSCs and PSCs have been widely proposed to be woven into powering textiles based on conventional weaving technology.[12–16] Although several attempts have been made to weave fiber-shaped solar cells into textiles, efficient solar cell textiles have not be realized thus far, mainly owing to damaging of the surface during the weaving process, short circuits during use, and very low energy conversion efficiencies. Furthermore, it has remained difficult to realize photovoltaic textiles with useful sizes by weaving of fiber-shaped solar cells.

Herein, an all-solid-state, lightweight, flexible, and wearable PSC textile with reasonable photovoltaic performance is developed. A metal textile electrode that was made from micrometer-sized metal wires is used as the cathode, and the surfaces of the metal wires were dip-coated with the photoactive layers. Two ultrathin, transparent, and aligned carbon nanotube (CNT) sheets that exhibit remarkable electronic and mechanical properties are coated onto the modifed metal textile at both sides as the anode to produce the desired PSC textile. Because of the designed sandwich structure, the PSC textiles displays almost the same energy conversion efficiencies regardless of which side it is irradiated from. As expected, the PSC textiles are highly flexible, and their energy conversion efficiencies varied by less than 3% after bending for more than 200 cycles. The PSC textile shows a low areal density of 5.9 mg cm$^{-2}$, compared to those of flexible film-based PSCs (31.3 mg cm$^{-2}$),[21] DSC textiles (173 mg cm$^{-2}$),[14] and PET/ITO-based solar cells (20 mg cm$^{-2}$).[7]

In a typical fabrication process (Figure 1), a titanium textile that had been woven from Ti wires and further modified with perpendicularly aligned $TiO_2$ nanotubes grown on their surfaces by electrochemical anodization was deposited with a layer of $TiO_2$ nanoparticles.[22] Two active layers of poly(3-hexylthiophene):phenyl-$C_{71}$-butyric acid methyl ester (P3HT:PCBM) and poly(3,4-ethyl-enedioxythiophene):poly(styrene sulfonate) (PEDOT:PSS) were sequentially dip-coated onto the modified Ti wires. Two flexible aligned CNT sheets were finally coated onto and adhered to both sides of the Ti textile to produce the PSC textile.

[*] Z. Zhang, X. Li, G. Guan, S. Pan, Prof. H. Peng
State Key Laboratory of Molecular Engineering of Polymers, Department of Macromolecular Science, and Laboratory of Advanced Materials, Fudan University
Shanghai 200438 (China)
E-mail: penghs@fudan.edu.cn
Z. Zhu, D. Ren
Key Laboratory for Ultrafine Materials of Ministry of Education, School of Materials Science and Engineering
East China University of Science & Technology
Shanghai 200237 (China)

[**] This work was supported by MOST (2011CB932503), NSFC (21225417), STCSM (12nm0503200), the Fok Ying Tong Education Foundation, the Program for Special Appointments of Professors at Shanghai Institutions of Higher Learning, and the Program for Outstanding Young Scholars from the Organization Department of the CPC Central Committee.

Supporting information for this article is available on the WWW under http://dx.doi.org/10.1002/anie.201407688.

  

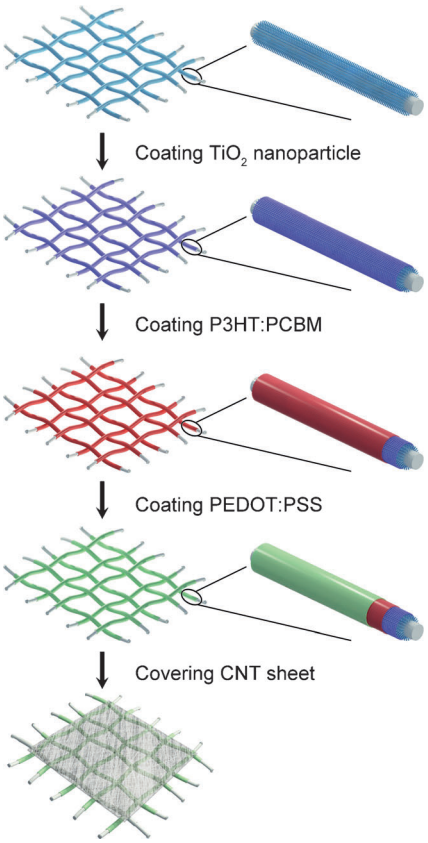


***Figure 1.*** Fabrication of the PSC textile.

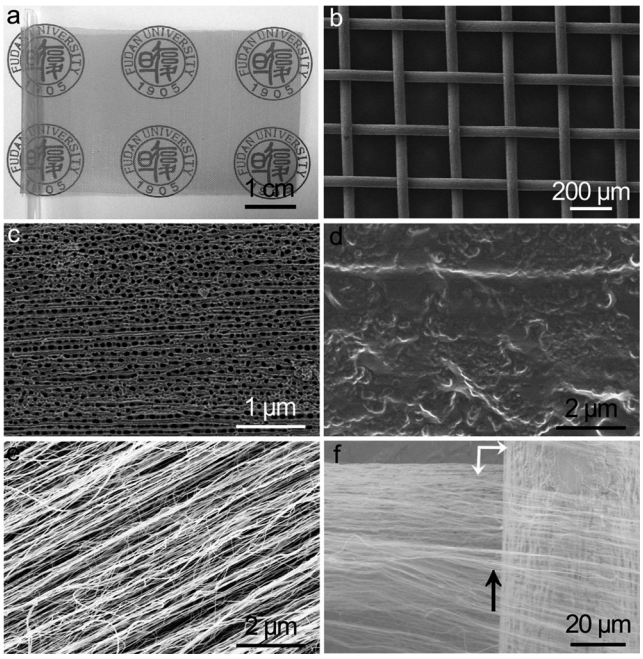


***Figure 2.*** a) Photograph of a Ti textile with one part wrapped around a glass rod and the other part on a labelled paper. b) SEM image of the Ti textile. c) SEM image of aligned $TiO_2$ nanotubes. d) Layers that were coated with P3HT:PCBM and PEDOT:PSS. e) Aligned CNT sheet. f) Aligned CNT sheet closely attached to the surface of the Ti textile. The white arrows indicate two crossed Ti wires while the black arrow indicates an aligned CNT sheet.

Importantly, the Ti textile was highly flexible, and a Ti textile with an area of $6.5 \times 3.5\ cm^2$ could be closely wrapped around a glass rod with a diameter of 3 mm without any damage (Figure 2a, left). The Ti textile showed an average thickness of appropriately 100 μm and was macroscopically transparent (Figure 2a, right) because of the uniform grid structure (Figure 2b; see also the Supporting Information, Figure S1). The diameters of the Ti wires were centered at 50 μm, and the average distance between two neighboring parallel Ti wires was 200 μm. Figure 2c shows a top view of the perpendicularly grown $TiO_2$ nanotubes with inner and outer diameters of 100 and 150 nm, respectively. The lengths of the $TiO_2$ nanotubes could be accurately controlled by varying the growth time during the electrochemical anodization. Aligned $TiO_2$ nanotubes were used to increase charge separation and transport in the PSC. A length of approximately 1.8 μm was found to produce the highest energy conversion efficiency and thus used in the following study (Figure S2). Shorter $TiO_2$ nanotubes could not be uniformly coated with the photoactive layers, whereas longer $TiO_2$ nanotubes led to increased diffusion pathways with lower energy conversion efficiencies.

Perpendicularly aligned $TiO_2$ nanotubes could serve as a more effective electron transfer layer than the nanoparticles. However, the aligned $TiO_2$ nanotubes featured a rugged surface, so it remained difficult to form thin, uniform photoactive polymer layers. To this end, a layer of semiconducting $TiO_2$ nanoparticles was introduced on the surface of the aligned $TiO_2$ nanotubes to make the outer surface more uniform, to increase the polymer load, and to decrease the electrical resistance for more efficient charge transport. Figure S3 shows a typical SEM image of $TiO_2$ nanoparticles on the surface of aligned $TiO_2$ nanotubes. The thickness of the $TiO_2$ nanoparticles was also critical to the photovoltaic performance and could be controlled by varying the treatment time. The optimized treatment time was found to be 30 minutes (Figure S4). A thinner $TiO_2$ nanoparticle layer was not effective at forming uniform surfaces and producing high polymer loads, whereas a thicker $TiO_2$ nanoparticle layer decreased the charge transport efficiency.

Thin and continuous P3HT:PCBM and PEDOT:PSS layers were sequentially formed on the outer surface of the modified Ti wire by dip coating (Figure 2d). The thicknesses of the P3HT:PCBM and PEDOT:PSS layers were calculated to be approximately 80 and 100 nm, respectively. The thickness of the polymer layer could be controlled by varying the concentration of the polymer solution and the coating times. Here, the PEDOT:PSS layer was used to improve hole transport, and it was transparent with a high optical transmittance so as not to prevent light from reaching the $TiO_2$ nanoparticle layer.

Figure 2e and f show SEM images of a typical aligned CNT sheet with a thickness of 18 nm. The aligned CNT sheet was dry-drawn from spinnable multi-walled CNT arrays that were synthesized by chemical vapor deposition (for details, see the Supporting Information and Figure S5).[23–26] The aligned CNT sheet was optically transparent with high transmittances over 80% and above 90% at wavelengths of

> 500 nm; the CNTs were also highly aligned to provide sheets with high electrical conductivities on the order of $10^2$ to $10^3$ S cm$^{-1}$,[27] so that the aligned CNT sheet can effectively collect holes from the PEDOT:PSS layer. A key reason for using aligned CNT sheets as electrodes is the fact that they are highly flexible and could be stably and closely attached to the surface of the modified Ti textile electrode (Figures S6 and S7 and Figure 2 f). SEM studies also confirmed that they would not peel off from the Ti substrate after bending for more than 200 cycles. The high transmittance and electrical conductivity render the aligned CNT sheet an effective electrode for the PSC textile.

The working mechanism of the PSC textile is summarized below.[28–30] Upon sunlight absorption, the heterojunction layer generates excitons, which are separated into holes and electrons. The holes are collected by the aligned CNT sheet anode from the PEDOT:PSS layer, while the electrons are transported to the Ti textile cathode through the $TiO_2$ layer. Based on the working mechanism, a systematic study on the dependence of the photovoltaic performance on the thickness of the aligned CNT sheet was carefully conducted to further optimize the PSC textile.

Figure S8 shows the optical transmittance spectra of aligned CNT sheets with increasing thicknesses from 18 to 36 to 54 nm, and their transmittances accordingly decreased from over 91 % to 83 % and 77 % at a wavelength of 550 nm. As a result, the open-circuit voltages remained almost unchanged while the short-circuit current densities decreased from 5.2 to 3.9 and 1.9 mA cm$^{-2}$ with the increasing thickness of the aligned CNT sheet (Figure 3 a). Although the resistances of the aligned CNT sheet (3 mm in width) decreased from 3.0 to 1.6 and 0.9 kΩ cm$^{-1}$ with the increase in thickness (Figures S9 and S10), for the thicker aligned CNT sheet, the transmission decreased with lower incident intensities for lower short-circuit current densities. The transmission dominated the PSC textile, so that the maximum energy conversion efficiency of 1.08 % occurred at 18 nm. Here, the effective irradiated area of the Ti textile was used to calculate the energy conversion efficiency of the PSC textile.

Both sides of the modified Ti textile had been coated with photoactive polymer layers and covered with the aligned CNT sheets, so that the energy conversion efficiencies of the unique PSC textile were almost the same (Figure 3 b). Figure 4 a and b show photographs of a PSC textile before and after bending. As expected, the PSC textile was flexible, and the energy conversion efficiencies varied by less than 3 % during 200 bending cycles (Figure 4 c). In Figure 4 d, *J–V* curves of a PSC textile before and after bending for 200 cycles are compared, and they almost overlap, which further demonstrates the high flexibility and stability. In addition, the aligned CNT sheet features excellent thermal and mechanical properties, so that a CNT coating on the outer surface provides the resulting PSC textile with a high stability during use. The high stability of the PSC textile was also confirmed by studying the energy conversion efficiencies with time. Over 92 % and 75 % of the energy conversion efficiency had been maintained after a period of ten days in argon and air, respectively (Figure S11 and S12).

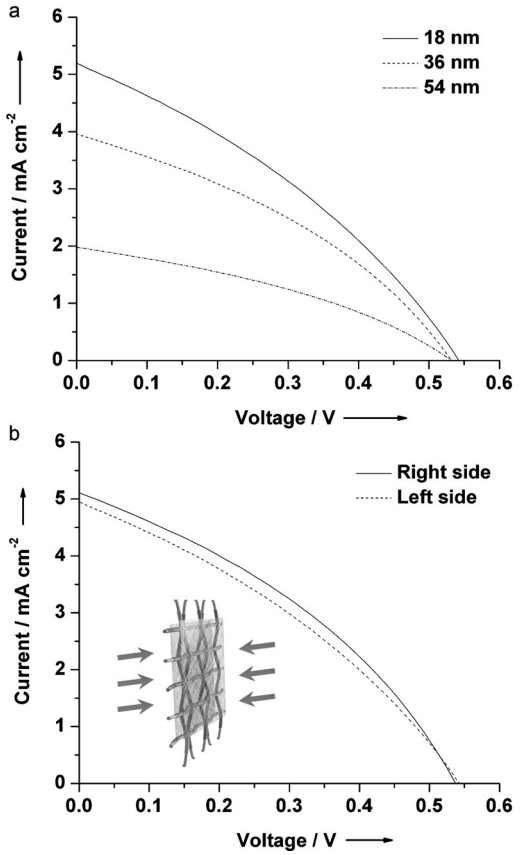


***Figure 3.*** a) *J–V* curves of the PSC textiles with an increase in the thickness of the aligned CNT sheets from 18 to 36 to 54 nm. b) *J–V* curves of a PSC textile with an aligned CNT sheet with a thickness of 18 nm.

In summary, a general and effective route for fabricating novel PSC textiles has been developed by sandwiching a metal textile electrode with two ultrathin, transparent, and conducting CNT sheets. The resulting PSC textile shows the same energy conversion efficiencies regardless of which side it is irradiated from because of its unique sandwich structure. The PSC textile is also highly flexible and stable, and the energy conversion efficiencies were well maintained after bending for 200 cycles. Furthermore, the PSC textile is lightweight and wearable, and can be integrated to power various portable electronic devices. More efforts are required to further enhance the energy conversion efficiency of the PSC textile by optimizing the structure, for example by increasing the contact area between the two electrodes.

## *Experimental Section*

Titanium wires with diameters of 50 μm were woven into textiles (100 mesh). The washing and preparation processes for the resulting Ti textile are described in the Supporting Information. Perpendicularly aligned $TiO_2$ nanotubes were then grown on the surface of the Ti textile electrode, followed by sequential deposition of the photoactive P3HT:PCBM and PEDOT:PSS layers. The aligned CNT sheet that served as the anode was finally coated onto the modified Ti textile electrode to produce the desired PSC textile. The aligned CNT sheet

  

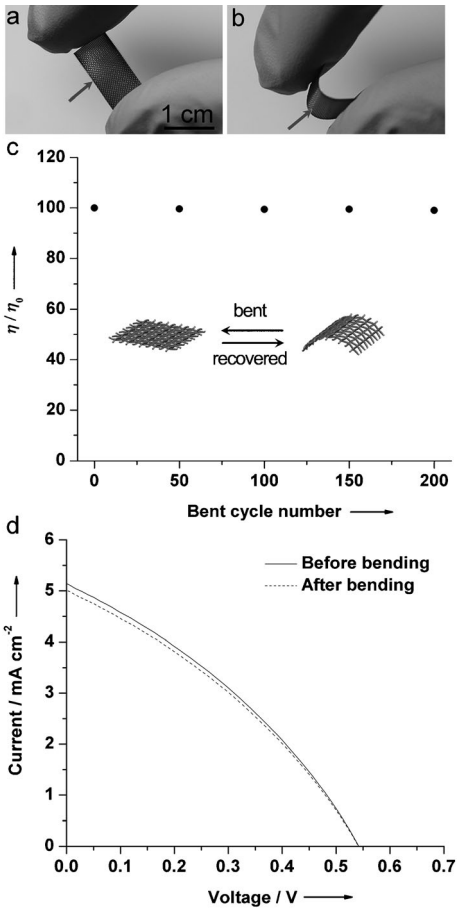


***Figure 4.*** a, b) and b) Photographs of the PSC textile before (a) and after (b) bending. c) Dependence of the energy conversion efficiency of the PSC textile on the bending cycle. $\eta_0$ and $\eta$ correspond to the energy conversion efficiencies before and after bending, respectively. d) *J–V* curves of the PSC textile before and after bending for 200 cycles.

had been dry-drawn from spinnable CNT arrays; this process is thoroughly discussed in the Supporting Information.

Received: July 28, 2014
Revised: August 10, 2014
Published online: August 26, 2014

**Keywords:** carbon nanotubes · electrochemistry · energy conversion · polymers · solar cells

[1] A. Sumboja, C. Y. Foo, X. Wang, P. S. Lee, *Adv. Mater.* **2013**, *25*, 2809.
[2] C. Choi, J. A. Lee, A. Y. Choi, Y. T. Kim, X. Lepró, M. D. Lima, R. H. Baughman, S. J. Kim, *Adv. Mater.* **2014**, *26*, 2059.
[3] K. Wang, W. Zou, B. Quan, A. Yu, H. Wu, P. Jiang, Z. Wei, *Adv. Energy Mater.* **2011**, *1*, 1068.
[4] L. Bao, J. Zang, X. Li, *Nano Lett.* **2011**, *11*, 1215.
[5] P. Docampo, J. M. Ball, M. Darwich, G. E. Eperon, H. J. Snaith, *Nat. Commun.* **2013**, *4*, 2761.
[6] A. Chirilă, S. Buecheler, F. Pianezzi, P. Bloesch, C. Gretener, A. R. Uhl, C. Fella, L. Kranz, J. Perrenoud, S. Seyrling, R. Verma, S. Nishiwaki, Y. E. Romanyuk, G. Bilger, A. N. Tiwari, *Nat. Mater.* **2011**, *10*, 857.
[7] B. Zhao, Z. He, X. Cheng, D. Qin, M. Yun, M. Wang, X. Huang, J. Wu, H. Wu, Y. Cao, *J. Mater. Chem. C* **2014**, *2*, 5077.
[8] S.-W. Heo, K.-W. Song, M.-H. Choi, T.-H. Sung, D.-K. Moon, *Sol. Energy Mater. Sol. Cells* **2011**, *95*, 3564.
[9] X. Fang, Z. Yang, L. Qiu, H. Sun, S. Pan, J. Deng, Y. Luo, H. Peng, *Adv. Mater.* **2014**, *26*, 1694.
[10] T. Chen, S. Wang, Z. Yang, Q. Feng, X. Sun, L. Li, Z.-S. Wang, H. Peng, *Angew. Chem. Int. Ed.* **2011**, *50*, 1815; *Angew. Chem.* **2011**, *123*, 1855.
[11] W. Guo, C. Xu, X. Wang, S. Wang, C. Pan, C. Lin, Z. L. Wang, *J. Am. Chem. Soc.* **2012**, *134*, 4437.
[12] Z. Yang, J. Deng, X. Sun, H. Li, H. Peng, *Adv. Mater.* **2014**, *26*, 2643.
[13] S. Hou, Z. Lv, H. Wu, X. Cai, Z. Chu, Yiliguma, D. Zou, *J. Mater. Chem.* **2012**, *22*, 6549.
[14] S. Pan, Z. Yang, P. Chen, J. Deng, H. Li, H. Peng, *Angew. Chem. Int. Ed.* **2014**, *53*, 6110; *Angew. Chem.* **2014**, *126*, 6224.
[15] S. Ito, S. M. Zakeeruddin, R. Humphry-Baker, P. Liska, R. Charvet, P. Comte, M. K. Nazeeruddin, P. Péchy, M. Takata, H. Miura, S. Uchida, M. Grätzel, *Adv. Mater.* **2006**, *18*, 1202.
[16] Q. Zhang, C. S. Dandeneau, X. Zhou, G. Cao, *Adv. Mater.* **2009**, *21*, 4087.
[17] D. Liu, M. Zhao, Y. Li, Z. Bian, L. Zhang, Y. Shang, X. Xia, S. Zhang, D. Yun, Z. Liu, A. Cao, C. Huang, *ACS Nano* **2012**, *6*, 11027.
[18] M. R. Lee, R. D. Eckert, K. Forberich, G. Dennler, C. J. Brabec, R. A. Gaudiana, *Science* **2009**, *324*, 232.
[19] T. Chen, L. Qiu, H. Li, H. Peng, *J. Mater. Chem.* **2012**, *22*, 23655.
[20] D. Liu, Y. Li, S. Zhao, A. Cao, C. Zhang, Z. Liu, Z. Bian, Z. Liu, C. Huang, *RSC Adv.* **2013**, *3*, 13720.
[21] D. J. Lipomi, B. C. K. Tee, M. Vosgueritchian, Z. Bao, *Adv. Mater.* **2011**, *23*, 1771.
[22] J. H. Yun, Y. H. Ng, C. Ye, A. J. Moze, G. G. Wallace, R. Amal, *ACS Appl. Mater. Interfaces* **2011**, *3*, 1585.
[23] L. Qiu, X. Sun, Z. Yang, W. Guo, H. Peng, *Acta Chim. Sin.* **2012**, *70*, 1523.
[24] Z. Zhang, Z. Yang, Z. Wu, G. Guan, S. Pan, Y. Zhang, H. Li, J. Deng, B. Sun, H. Peng, *Adv. Energy Mater.* **2014**, DOI: 10.1002/aenm.201301750.
[25] Z. Zhang, X. Chen, P. Chen, G. Guan, L. Qiu, H. Lin, Z. Yang, W. Bai, Y. Luo, H. Peng, *Adv. Mater.* **2014**, *26*, 466.
[26] X. Sun, Z. Zhang, X. Lu, G. Guan, H. Li, H. Peng, *Angew. Chem. Int. Ed.* **2013**, *52*, 7776; *Angew. Chem.* **2013**, *125*, 7930.
[27] H. Peng, X. Sun, F. Cai, X. Chen, Y. Zhu, G. Liao, D. Chen, Q. Li, Y. Lu, Y. Zhu, Q. Jia, *Nat. Nanotechnol.* **2009**, *4*, 738.
[28] Z. He, C. Zhong, S. Su, M. Xu, H. Wu, Y. Cao, *Nat. Photonics* **2012**, *6*, 1.
[29] M. Ye, X. Xin, C. Lin, Z. Lin, *Nano Lett.* **2011**, *11*, 3214.
[30] G. Li, R. Zhu, Y. Yang, *Nat. Photonics* **2012**, *6*, 153.